View Article Online / Journal Homepage / Table of Contents for this issue

Organic & Biomolecular Chemistry

Dynamic Article Links

Cite this: *Org. Biomol. Chem.*, 2011, **9**, 1972

www.rsc.org/obc

PAPER

Functionalized guanidinium chloride based colourimetric sensors for fluoride and acetate: single crystal X-ray structural evidence of -NH deprotonation and complexation†

Purnandhu Bose, B. Nisar Ahamed and Pradyut Ghosh*

Received 28th October 2010, Accepted 17th November 2010
DOI: 10.1039/c0ob00947d

Published on 24 January 2011 on http://pubs.rsc.org | doi:10.1039/C0OB00947D
Downloaded by University of Sussex on 06 January 2013

A series of new symmetrically functionalized guanidinium chlorides (**S1–S10**) are synthesized in good yields and their sensing ability toward anions is studied in MeCN–DMF (24 : 1) (v/v). The absorption bands of these molecules in the presence of anions are tuned by varying the functional groups attached to the guanidinium moiety (which resembles urea) with respect to (i) aromaticity (**S1–S4**), (ii) electron induction effect (**S1**, **S5–S9**), (iii) positional isomeric effect (**S7–S9**), (iv) indole functionality (**S10**) of the conjugated aryl units. Anions that are above Cl^- in the Hofmeister series (F^-, AcO^-, $H_2PO_4^-$) are eligible as an analyte in this series of molecules whereas less basic anions than Cl^- do not cause any interference. Thus, this series of molecules are suitable for the detection of anions in the narrow window of the Hofmeister series. Out of all the anions, only fluoride causes vivid colour changes from yellow to red to reddish orange and finally to blue, irrespective of the increasing aromaticity, induction and positional isomeric effect of the substituent that is attached to the guanidinium moiety. Interestingly, **S9** has shown the ability to sense distinctly both F^- and AcO^- colourimetrically. Further **S10**, a sensor attached with indole functionality shows selective sensing of F^- colourimetrically with a NIR signature at ~930 nm though both these outputs are very unstable in nature. Stability constants for complex formation of **S1–S10** (except **S5**) with F^-, AcO^- are calculated by UV–vis titration experiments. Finally single crystal X-ray structural studies on the species **1** formed upon treating **S6** with sodium fluoride confirms -NH deprotonation, whereas the reaction of **S6** and **S2** with sodium benzoate shows 1 : 1 host : guest binding that results in complexes **2** and **3** respectively.

Introduction

Anions like fluoride, acetate and phosphate play major roles in a wide range of chemical and biological systems and sometime they are of environmental concern.[1] For example, fluoride, is of special interest due to its applications in industry, food and toxicity.[2] Whereas carboxylate anions exhibit specific biochemical behaviors in enzymes and antibodies and are also critical components of numerous metabolic processes. On the other hand, phosphate is one of the key ingredients in the fertilizer industry. Therefore, receptors capable of sensing these anions are of crucial importance.[3] Recently, considerable efforts have been made to develop colourimetric molecular probes for different anionic guests.[4] The colourimetric probes are attractive for their "naked eye" detection of target species and offer qualitative and quantitative information using inexpensive equipment.[5] Many synthetic receptors having pyrrole/calixpyrrole,[2b,m,p] amide,[2a,c,o] urea,[2g,h,i] thiourea,[2e,f,g] bisthiocarbonohydrazone[2q,r] dipyrrolylquinoxaline,[2k,n,d] and indolocarbazole[2j,l] moieties for colourimetric sensing of inorganic anions have been reported. In most of the amide, urea and thiourea based systems, the intense colouration in the presence of fluoride in solution is explained *via* deprotonated receptors and its delocalization but solid state structural evidence of deprotonated species are rare.[3] Resembling urea and thiourea, the guanidinium recognition element is widely distributed as an anion binding site in biology as well as in synthetic anion receptor designs.[4] In the recent past, Schmuck[5] *et al.* and Anslyn[5] *et al.* have shown detection of citrate using guanidinium based tripodal receptors but use of guanidinium based receptors for the sensing of inorganic anions is limited.[6] Recently, Zhao *et al.*[2q] and we[2r] have established thiocarbonohydrazones as efficient colourimetric anion sensors which are easy to synthesize. Our work on indole conjugated bisthiocarbonohydrazone/biscarbonohydrazone systems shows these ligands as efficient colourimetric anion sensors that allow selective detection of fluoride by the naked eye, with a characteristic NIR signal

Department of Inorganic Chemistry, Indian Association for the Cultivation of Science, 2A&2B Raja S. C. Mullick Road, Kolkata 700 032, India. E-mail: icpg@iacs.res.in; Fax: (+91) 33-2473-2805

† Electronic supplementary information (ESI) available: ^{1}H NMR, ^{13}C NMR and ESI-MS spectrum of **S1–S10**. Selectivity investigation and UV–vis titration experiment of **S1–S10** in the presence of different anions. CCDC reference numbers 775864, 795757 and 782762. For ESI and crystallographic data in CIF or other electronic format see DOI: 10.1039/c0ob00947d

This journal is © The Royal Society of Chemistry 2011

Published on 24 January 2011 on http://pubs.rsc.org | doi:10.1039/C0OB00947D
Downloaded by University of Sussex on 06 January 2013

at more than 900 nm.[2r] Herein, we introduce a series of newly synthesized guanidinium chloride salt based conjugated systems (having different conjugation or electron withdrawing ability of the attached aryl moiety, Scheme 1) as efficient colourimetric and selective sensors for F^- *via* naked eye detection of a pattern of colour changes as well as wide ranges of absorption signals that include NIR signature, across the series. We have also shown the colourimetric sensing of fluoride and acetate by one of the receptors in the series. Moreover, structural evidence of –NH deprotonation by fluoride *vs.* binding of benzoate with the receptors in the series are also established.

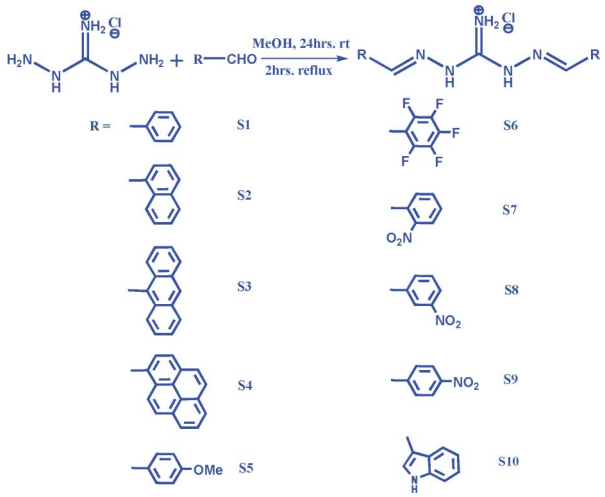

Scheme 1 Synthesis of colourimetric anion sensors **S1–S10**.

Results and discussion

In this article we have synthesized a series of new guanidinium based receptors for anion sensing studies. This series of receptors belongs to the functionalized guanidinium chloride salts. Thus, anions having higher basicity than Cl^- like F^-, HSO_4^-, AcO^- and $H_2PO_4^-$ might act as analytes for colourimetric sensing by this series of sensors. These sensor molecules are thoroughly characterized by ^{1}H-NMR, ^{13}C-NMR, ESI-MS and elemental analyses. The main features of these molecules are as follows: (1) they can be easily synthesized by simple Schiff base condensation reaction between *N*,*N*′-diaminoguanidine hydrochloride and the corresponding aldehyde in good yields; (2) the guanidinium moiety is very important in biological systems. In the biological world the guanidinium moiety is widely distributed as a mediator of specific non-covalent binding; (3) anions which are below Cl^- in the Hofmeister series are expected not to interfere in the sensing studies; (4) indole functionalized guanidinium system could act as a NIR probe for fluoride as observed in cases of indole conjugated bisthiocarbonohydrazone/biscarbonohydrazone systems.[2r]

This series of sensor molecules (**S1–S10**) can be categorized into four sub-series based on (i) aromaticity (**S1–S4**), (ii) electron induction effect (**S1**, **S5–S9**), (iii) positional isomeric effect (**S7–S9**) and (iv) indole functionality (**S10**) of the conjugated aryl units. In the following sections we describe the effect of each category on the sensing aspect of anions *via* solution and solid state studies.

Solution state study

In the first part of our discussion, we focus on the colourimetric changes of molecules (**S1–S9**) in the presence of different anions: F^-, Cl^-, Br^-, I^-, NO_3^-, AcO^-, $H_2PO_4^-$. **S10** along with its thiourea and urea analogues are studied separately in the later part of our discussions. Fig. 1 shows distinct colour changes for **S1–S9** in the presence of F^-. Fluoride causes drastic colour changes from yellow to red to reddish orange and finally to blue irrespective of the increasing aromaticity, induction and positional isomeric effect of the substituent attached to the guanidinium moiety (Fig. 1). Fluoride also causes similar colour changes in the series in the presence of other anions. Thus, this series of molecules selectively detects F^- over other anions colourimetrically.

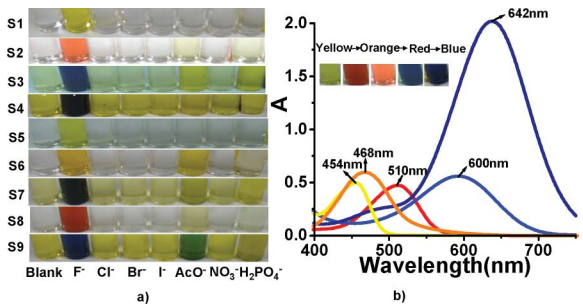

Fig. 1 a) Colour changes observed upon addition of 3×10^{-3} M anions to MeCN–DMF (9.6 : 0.4) (v/v) solution of 1×10^{-4} M ligands. b) Selective spectral change of selective sensor molecules in the presence of F^- ion (Yellow - **S1**, Orange - **S8**, Red - **S2**, Blue - **S3**, Deep blue - **S9**).

The optical properties of (**S1–S4**) in the presence of tetrabutylammonium $(n\text{-}Bu_4N)^+$ salts of different anions were studied in detail. Only in the presence of F^- is a colourless to yellow colouration (Fig. 1), and corresponding change in optical spectrum (Fig. 2a), observed in the case of phenyl substituted system **S1**. The absorption peak at 346 nm of **S1** is mainly due to the Ar–CH═N–NH conjugation framework. In the presence of F^- the above peak diminishes, with the appearance of a new absorption peak at around 454 nm. Most of the reported chemosensors based on urea and amide functionality show almost similar colour changes with F^-, AcO^- and $H_2PO_4^-$ due to their close basic nature. The F^- selective colour change in this case could be due to the guanidinium moiety having positive charge on the central nitrogen which favours the selective interaction of spherical and basic F^- *via* electrostatic interaction, even though it possesses favourable binding site (V shaped) for AcO^-, $H_2PO_4^-$.

Moving from phenyl to naphthyl substitution, **S2**, the aromaticity increases to some extent and as a result the absorption peak appears at around 378 nm (Fig. 2b). The colour of the sensor molecule in the presence of F^- changes to red with λ_{max} at 510 nm whereas the effect of other anions is insignificant. Upon increasing the conjugation by introducing anthracene and pyrene moieties, the optical spectra of **S3** (λ_{max} at 420 nm) and **S4** (λ_{max} at 440 nm) shifted to 600 and 604 nm respectively (Fig. 2c & 2d) in the presence of F^-. In both the cases, colour changes from yellow to blue are observed (Fig. 1). From these studies it is clear that with the increase in the aromaticity of the substituent attached to the guanidinium unit, the peaks corresponding to λ_{max} of the molecules in the presence of F^- shift from 454 nm to 604 nm *i.e.* a tuning of

Published on 24 January 2011 on http://pubs.rsc.org | doi:10.1039/C0OB00947D
Downloaded by University of Sussex on 06 January 2013

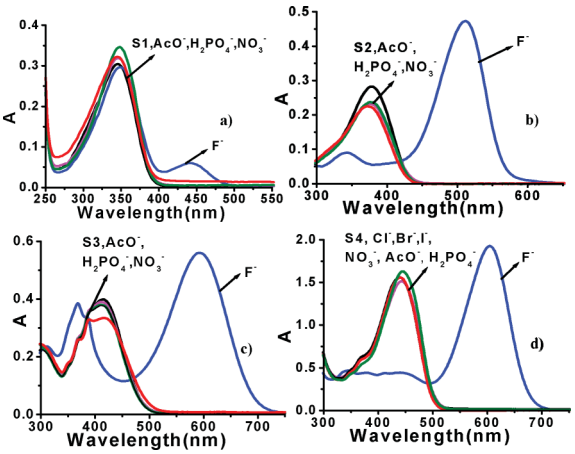

Fig. 2 Changes in the UV–vis absorption spectra a)-d) of **S1–S4** (1.0×10^{-4} M) in MeCN–DMF (9.6 : 0.4) (v/v) solution upon addition of 50 equiv. of different anions.

colouration from yellow to red to blue could be obtained in the presence of F^- (Fig. 1). The pattern of selective colour changes of **S1–S4** by F^- could be useful as a unique signature toward the detection of F^-.

The optical properties of **S5–S9** along with **S1** in the presence of different anions were studied to understand the electron induction effect of the conjugated substituents in the series. In **S5** having 4-methoxy phenyl substituent the electron donating group makes the proton of the -NH group of the guanidinium moiety less acidic and as a result the interaction with anion is expected to be less than that of **S1**. Although the colour change as well as the wavelength shift in the presence of F^- in **S5** is almost similar to that of phenyl substituted **S1** molecule (Fig. 1, Figure S31, ESI†). Both **S1** and **S5** show colour change only in the presence of F^- among the different anions tested in this study. When phenyl substitution in **S1** is replaced by pentafluorophenyl moiety, the ligand **S6** shows a change in colour from colourless to yellow with both F^- and AcO^- (Fig. 1) but $H_2PO_4^-$ fails to generate such a colour change. This indicates that other than the basicity, geometry of the anions also plays an important role in the interaction of anions with the guanidinium moiety. Colour change in the presence of AcO^- with **S6** could be due to its planar geometry where the V shaped guanidinium binding site allows its possible interactions and is further justified by the single crystal structure of **S6** with benzoate, which is explained in the later part of our discussion.

Three other sensor molecules (**S7–S9**) in this series were synthesized by replacing the phenyl group of **S1** with $–NO_2$ substituted phenyls to introduce electron withdrawing effect as well as to see the positional isomeric effects on the anion sensing. Molecule **S7** with 2-substituted $–NO_2$ shows a light yellow colouration with a λ_{max} at 324 nm (Table 1). In the presence of F^-, **S7** shows a characteristic dark blue colour corresponding to 588 nm (Fig. 1, Figure S31c, ESI†) which could be due to the deprotonation of –NH and its stabilization through delocalization. It is further surprising that none of the anions $AcO^-/H_2PO_4^-$ do cause such a colour change in the similar experimental conditions (Fig. 1). In the case of **S8** where the $–NO_2$ is in the *meta* position, the –NH proton of the guanidinium moiety is less acidic compared to that in the *ortho* and *para* isomers. As a result, **S8** shows a selective colour change from colourless to orange red (468 nm) only in

Table 1 Binding or deprotonation constants and absorption maxima of the sensors with anions in MeCN–DMF (24 : 1) (v/v) solution, at 25 °C[a]

Sensor	F^- Log K	AcO^- Log K	Only Sensor (nm)	With F^- (nm)	With AcO^- (nm)
S1	2.42	—[b]	346	454	346
S2	1.69	2.62	378	510	428
S3	3.20	3.08	420	600	478
S4	2.51	2.77	440	604	473
S5	—	—[b]	354	456	354
S6	4.57	3.13	346	468	454
S7	2.27	—[b]	324	588	584
S8	2.10	—[b]	304	468	362
S9	4.17	3.60	346	642	642
S10	3.18[c]	—[b]	354	932	354
S11	3.80[d]	—[b]	342	936	342
S12	2.48[d]	—[b]	314	904	314

[a] 1.0×10^{-5} (M) of sensor in MeCN–DMF (24 : 1)(v/v) solution. Constants determined by fitting a 1 : 1 binding model. For most of the cases determination coefficients r^2 is > 0.98. [b] No spectral changes were observed or the minor change was not suitable for accurate measurement of the log K values. [c] Titration experiment was carried out in UV–vis diode array. [d] Values obtained from ref. 2r.

the presence of F^- (Fig. 1, Figure S31d, ESI†). The *para* isomer, **S9** shows two distinct colour changes yellow (λ_{max} at 346 nm) to blue (λ_{max} at 642 nm) and green (λ_{max} at 642 nm) for F^- and AcO^- respectively, whereas $H_2PO_4^-$ maintains its lesser reactivity toward the guanidinium –NH, causing a negligible colour change (Fig. 1). In the presence of AcO^- and $H_2PO_4^-$ similar colour change is observed for F^- whereas AcO^- shows its characteristic green colour even in the presence of $H_2PO_4^-$ (Figure S33, ESI†). In the case of **S9** the 4-substituted $–NO_2$ can exert both –I as well as –R effects and this increases the acidity of the –NH proton of the guanidinium moiety. A huge red shifted strong absorption peak at 642 nm (>200 nm shift) ($\varepsilon_{642\,nm} = 29\,017\ M^{-1}\ cm^{-1}$) is observed along with an enormous decrease in the peak intensity corresponding to the n–π* transition of the ligand in the presence of F^- (Fig. 3a). This molecule also shows a distinct green colouration. The optical spectrum demonstrates a low intense peak at 642 nm ($\varepsilon_{642\,nm} = 2805\ M^{-1}\ cm^{-1}$) in the presence of AcO^- (Fig. 3b). Thus, the difference in colour in the cases of F^- and AcO^- could be due to the difference in molar extinction coefficient values (Fig. 3b). Fig. 4 illustrates the colour gradient experiments with **S9** (1×10^{-5} M) in the presence of various equivalents of F^- and AcO^-. Upon addition of different equivalents of F^- the colour changes from yellow to green and finally to blue whereas in the presence of AcO^- the colour transforms from yellow to green and it never attains the blue colouration even after 1000 equivalents of anion. Distinct colour changes are observed in the case of **S9** (1×10^{-5} M) in the presence of 20 and 50 equivalents of F^- and AcO^- respectively. When the concentration of **S9** is increased from (1×10^{-5} M) to (2.5×10^{-5} M), characteristic colour changes for F^- and AcO^- are observed with the addition of 2.5 equivalents of anions (Fig. 5). Thus in both these cases the colorimetric detection limit of these anions is estimated to ~6.25×10^{-5} M. In the case of $H_2PO_4^-$ an intensified yellow colouration is observed with **S9** (Fig. 1) though it is more basic than AcO^-. The slight change in colour in the case of $H_2PO_4^-$ is due to the weak absorption peak at 642 nm ($\varepsilon_{642\,nm} = 1089\ M^{-1}\ cm^{-1}$). It is surprising that none of the sensor molecules do show prominent colour change in the case of one of the most basic anions, $H_2PO_4^-$. Thus **S9** could be used to

 This journal is © The Royal Society of Chemistry 2011

Published on 24 January 2011 on http://pubs.rsc.org | doi:10.1039/C0OB00947D
Downloaded by University of Sussex on 06 January 2013

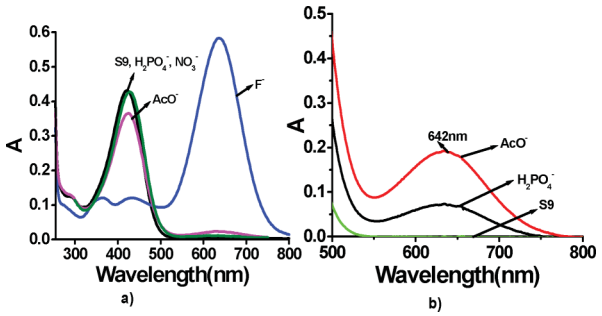

Fig. 3 a) Changes in the UV–vis absorption spectrum of **S9** (1.0×10^{-5} M) in MeCN–DMF (9.6 : 0.4) (v/v) solution upon addition of 50 equiv. of anions. b) Optical spectrum of 6.7×10^{-5} M of **S9** and **S9** in the presence of 30 equiv. of AcO^- or $H_2PO_4^-$.

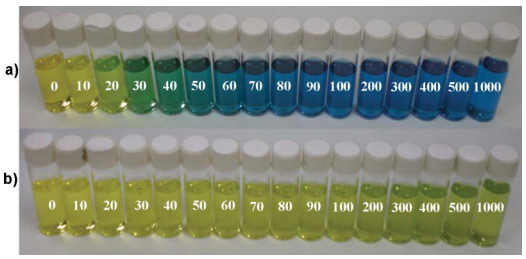

Fig. 4 Colour gradient experiment of **S9** (1×10^{-5} M) in the presence of various equivalents of F^- (a) and AcO^-(b) respectively.

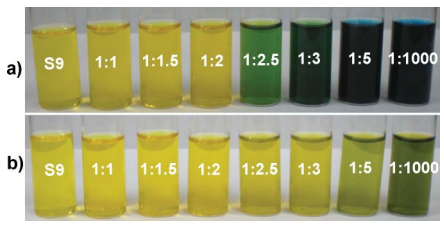

Fig. 5 Colour gradient experiment of **S9** (2.5×10^{-5} M) in the presence of various equivalents of F^- (a) and AcO^-(b) respectively.

differentiate generally three commonly behaving anions F^-, AcO^- and $H_2PO_4^-$ colourimetrically.

We have studied the binding interactions of sensors in the presence of F^- and AcO^- using UV–vis titration experiments (Table 1). Fig. 6a shows UV–vis titration of **S1** with F^-. It is evident from this titration that with the gradual increase of F^- concentration, the absorption peak at 346 nm decreases gradually with concomitant development of a new absorption peak at around 454 nm with one clear isosbestic point at around 376 nm. This indicates there are two species are in the equilibrium. The titration reaches saturation limit at 3.5×10^{-3} (M) concentration of F^- (Fig. 6b). The log K of this system is calculated to be 2.42 by using the Benesi–Hildebrand equation (Table 1, Figure S34, ESI†). Similarly, Fig. 7 and 8 demonstrate the UV-Vis titration experiments of **S9** with F^- and AcO^- respectively. For both these anions the absorption peak at 346 nm systematically decreases whereas a new absorption peak at around 642 nm rises with gradual increment of anion concentration. In the case of F^-, a clear isosbestic point is observed at 478 nm whereas for AcO^- it appears at 460 nm respectively. The calculated deprotonation/binding constants of F^- and AcO^- are tabulated in Table 1.

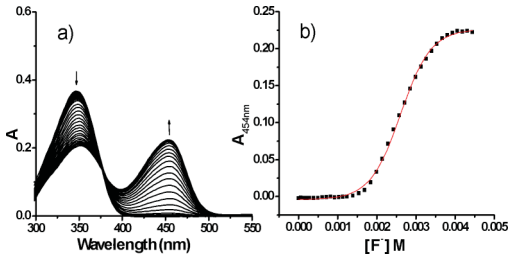

Fig. 6 **a**) UV–vis titration of the sensor **S1** (1.0×10^{-5} M) in MeCN–DMF (9.6 : 0.4) (v/v) solution with standard 0.01(M) solution of $[Bu_4N]F$; b) Absorption of sensor **S1** at 454 nm *vs.* concentration of fluoride anion.

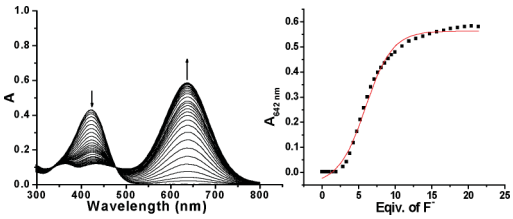

Fig. 7 **a**) UV–vis titration of the sensor **S9** (1.0×10^{-5} M) in MeCN–DMF (9.6 : 0.4) (v/v) solution with standard 0.01(M) solution of $[Bu_4N]F$; b) Absorption of sensor **S9** at 642 nm *vs.* equivalent of fluoride anion.

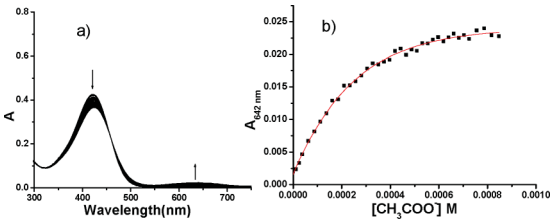

Fig. 8 **a**) UV–vis titration of the sensor **S9** (1.0×10^{-5} M) in MeCN–DMF (9.6 : 0.4)(v/v) solution with standard 0.01(M) solution of $[Bu_4N]AcO$; b) Absorption of sensor **S9** at 642 nm *vs.* equivalent of acetate anion.

We have also synthesized indole conjugated guanidinium chloride based sensor molecule **S10**. It resembles the urea and thiourea based sensor molecules **S11** and **S12** (Scheme 2).[2r] The characteristic feature of **S10** is that it can selectively sense F^- by naked eye detection of selective colour change from colourless (with an absorption peak at 354 nm due to the Ar–CH═N–NH conjugation framework, Figure S32, ESI†) to pink (Fig. 9) with a characteristic absorption band at 932 nm in acetonitrile/dimethyl formamide 9.6 : 0.4 (v/v) (Figure S32, ESI†), like previously reported systems **S11** and **S12**. In the presence of F^- **S10** shows three distinct peaks at 514, 564 and 932 nm. To the best of our knowledge a sensor with a huge red-shifted (~600 nm) NIR signal at more than 900 nm in the presence of F^- is rare (Figure S32, ESI†).[2r] The drawback of **S10** is the very unstable nature of the pink colour in the presence of F^-. The pink colour observed in this case (Fig. 9) rapidly turns to colourless whereas the pink

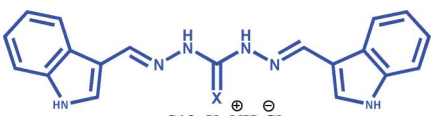

S10: X=NH_2Cl
S11 : X=S
S12 : X=O

Scheme 2 Structure of chemosensors **S10–S12**.

Published on 24 January 2011 on http://pubs.rsc.org | doi:10.1039/C0OB00947D
Downloaded by University of Sussex on 06 January 2013

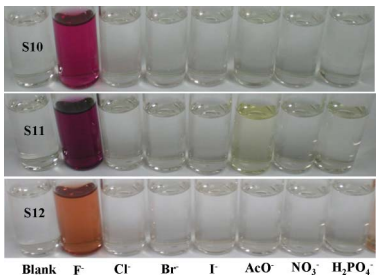

Fig. 9 Colour changes observed with the addition of different anions (~30 equivalents) to MeCN–DMF (9.6 : 0.4) (v/v) solution of 10^{-4} M **S10–S12**.

colouration observed in the cases of **S11** and **S12** is quite stable in our experimental conditions. This could be due to easy proton uptake ability from atmospheric moisture by the deprotonated species of **S10** compared to the cases of **S11** and **S12**. We have monitored the effect of atmospheric moisture toward the colour stability of the above cases optically as well as by absorption studies (Fig. 10). Clearly evident is the quite stable nature of the colour-adducts in the cases of **S11** and **S12** with F^- (Fig. 10b and 10c) but the very unstable nature of the species in the case of **S10** (Fig. 10a). In fact within 5 min (blue spectrum, Fig. 10a) 90% reduction of peaks intensity is observed and peaks at 514, 564 and 932 nm completely vanish within 15 min. The UV–vis titration experiment of **S10** in the presence of standard solution of F^- ion is carried out using UV–vis diode array. The calculated deprotonation or binding constant value is log K = 3.18 whereas in the cases of **S11** and **S12** values are 3.80 and 2.48 respectively (Table 1). Of course the value obtained in the case of **S10** could be more erroneous due to the unstable nature of the species formed in the presence of F^-.

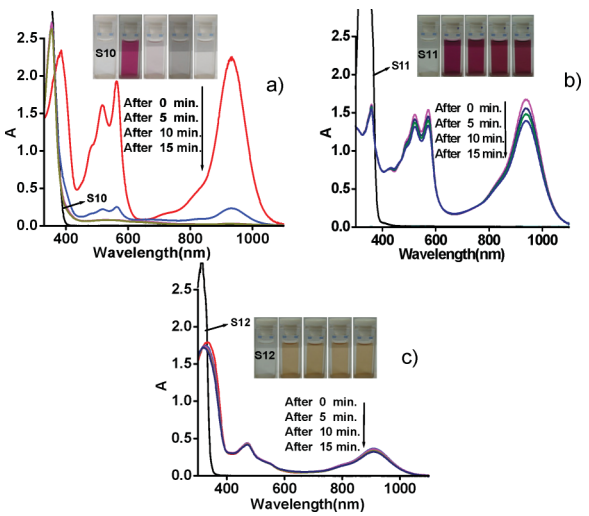

Fig. 10 Time dependent monitoring of colour changes of 1×10^{-4} M of ligand in the presence of 30 equivalents of F^- for (a) **S10**, (b) **S11**, (c) **S12**. Readings are taken at 5 min intervals.

Solid state study

Efforts were made to isolate single crystals of the complexes formed by ligands **S1–S10** upon reacting with F^-, AcO^-, $H_2PO_4^-$ and $PhCO_2^-$ salts respectively. Upon several attempts we were able to isolate single crystals of **S6** in the presence of NaF

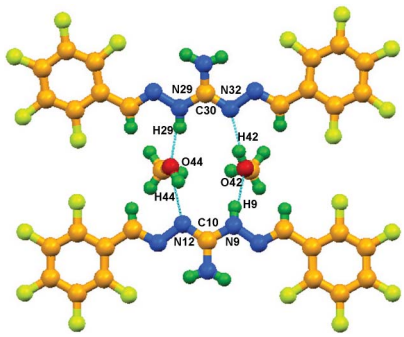

Fig. 11 Single crystal X-ray structure of deprotonated species **1** (Orange: C; deep green: H; blue: N; red: O; light green: F.)

i.e. deprotonated compound **1** and complexes **2** and **3** in the presence of $PhCO_2Na$ with **S6**, **S2** in MeOH respectively.‡ Single crystal X-ray structural analysis of **1** shows the evidence of zwitterionic species generated from the hydrochloride salt of **S6** upon extraction of one –NH proton of the guanidinium moiety followed by removal of counter anion *i.e.* Cl^- (Fig. 11). Deprotonated –NH in **1** is identified from the N–C bond distances. The N(12)–C(10) and N(32)–C(30) distances are 1.338 Å and 1.322 Å respectively which are significantly shorter than the N(9)–C(10) and N(29)–C(30) distances 1.366 Å and 1.361 Å respectively. Shorter distances in N(12)–C(10) and N(32)–C(30) are due to the development of partial double bond character after the deprotonation and its delocalization. In **1** two molecules are intermolecularly hydrogen bonded by two MeOH molecules *via* N–H···O and O–H···N interactions respectively as shown in Fig. 11. The detailed hydrogen bonding interactions are given in the ESI† (Table S2). Solid state structural evidence of mono deprotonation of the guanidinium moiety is also in agreement with the UV–vis titration profile of **S6** (Figure S43, ESI†) in the presence of F^- where a clear single isosbestic point at 394 nm is observed. In the case of complex **2**, single crystal X-ray structural analysis shows the formation of a 1 : 1 complex of **S6** and benzoate (where Cl^- is replaced by $PhCOO^-$) (Fig. 12). The carboxylate group of benzoate ion is hydrogen bonded with guanidinium –NH protons *via* N–H···O interactions (Fig. 12, Table S3, ESI†). In addition to the benzoate interaction with the guanidinium –NH proton, benzoic acid units (could be formed by uptake of

‡ *Crystallographic data* for **1**: $C_{16}H_9F_{10}N_5O$, M_r = 477.28, Monoclinic, space group $P2_1/n$, a = 16.012(10), b = 11.932(7), c = 19.682(12) Å, α = 90.00, β = 104.571(8), γ = 90.00°, V = 3639(4) Å^3, Z = 8, ρ_{calcd} = 1.742 g cm^{-3}, μ = 0.184 mm^{-1}, T = 120(2) K, 23147 reflections, 5944 independent (Rint. 0.0554), and 3922 observed reflections [$I > 2\sigma(I)$], 633 refined parameters, R_1 = 0.0499, wR_2 = 0.1123, GOF = 1.022. Complex **2**: $C_{36}H_{22}F_{10}N_5O_6$, M_r = 810.59, Monoclinic, space group $P2_1/m$, a = 6.8654(13), b = 34.567(6), c = 7.1380(14) Å, α = 90.00, β = 98.565(4), γ = 90.00°, V = 1675.1(5) Å^3, Z = 2, ρ_{calcd} = 1.607 g cm^{-3}, μ = 0.148 mm^{-1}, T = 100(2) K, 15838 reflections, 3005 independent (Rint. 0.0375), and 2607 observed reflections [$I > 2\sigma(I)$], 232 refined parameters, R_1 = 0.0334, wR_2 = 0.0842, GOF = 1.078. Complex **3**: $C_{37}H_{31}N_5O_4$, M_r = 609.67, Orthorhombic, space group *Pbca*, a = 14.5032(10), b = 9.6882(7), c = 44.522(3) Å, α = 90.00, β = 90.00, γ = 90.00°, V = 6255.7(8) Å^3, Z = 8, ρ_{calcd} = 1.295 g cm^{-3}, μ = 0.086 mm^{-1}, T = 100(2) K, 55819 reflections, 5518 independent (Rint. 0.0437), and 4635 observed reflections [$I > 2\sigma(I)$], 417 refined parameters, R_1 = 0.0879, wR_2 = 0.2308, GOF = 1.161. CCDC 775864, CCDC 795757 and CCDC 782762 contain the supplementary crystallographic data for **1**, Complex **2** and Complex **3** respectively. These data can be obtained free of charge from The Cambridge Crystallographic Data Centre *via* www.ccdc.cam.ac.uk/data_request/cif.

This journal is © The Royal Society of Chemistry 2011

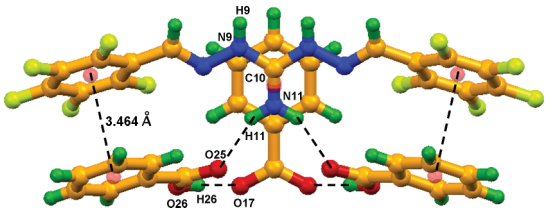

Fig. 12 Single crystal X-ray structure of complex **2** showing the interaction of the guanidinium moiety with a benzoate anion and two benzoic acid units *via* hydrogen bonding, π···π stacking and cation···π interactions. (Orange: C; deep green: H; blue: N; red: O; light green: F.)

proton from the solvent by benzoate during crystallization) are also in hydrogen bonding interaction with the benzoate ion as well as with the guanidinium moiety (Fig. 12). Further, the electron deficient pentafluoro ring of the guanidinium ligand and the electron rich phenyl ring of the benzoic acid unit are in π···π stacking interaction with a centroid···centroid distance of 3.464 Å (Fig. 12). Again the delocalised guanidinium cationic unit is in cation···π stacking interaction with the π-cloud of the benzoate ion. The distance between the centroid of C(10)=N(11) of the guanidinium unit and the centroid of the phenyl ring of benzoate is 3.269 Å (Fig. 13).

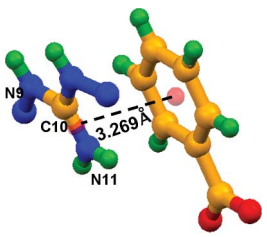

Fig. 13 Close-up view of the molecular association *via* cation···π stacking among the guanidinium cation and π- cloud of benzoate ion.

This type of solid state structural evidence of cation···π stacking interaction is rare[7] and mostly found in arginine based protein structures where the guanidinium moiety is the active site for binding interaction with carboxylate group. This π-stacked guanidinium ion probably enhances the binding ability of benzoate with **S6** in complex **2**. Ligand **S2** is also involved in the complex formation with $PhCO_2Na$ in a somewhat different fashion, which is shown by the complex **3** (Fig. 14, Table S4, ESI†). In this complex the carboxylate group of benzoate is perfectly hydrogen bonded with the guanidinium –NH protons *via* N–H···O interaction as in the case of complex **2**. In addition to that, one benzoic acid moiety is also in hydrogen bonding interaction with one of the oxygens of the carboxylate group of benzoate *via* O–H···O(benzoate) (Fig. 14). The O(2)–H(3X)···O(3)(benzoate) bond distance and angle are 2.600 Å and 173.8° respectively.

The detailed hydrogen bonding interactions for complexes **2** and **3** are given in ESI† (Table S3 and S4). Also there is no significant colour change of **S1–S10** in the presence of benzoate, suggesting interactions of these ligands with benzoate is solely binding phenomenon.

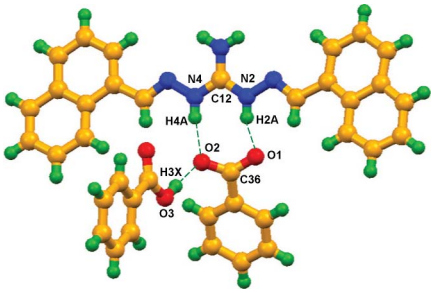

Fig. 14 Single crystal X-ray structure of complex **3** where a benzoate ion is attached in 1 : 1 fashion with the guanidinium moiety. In addition to that one benzoic acid unit is also present. (Orange: C; deep green: H; blue: N; red: O.)

Experimental

N,*N*′-diaminoguanidine hydrochloride and all tetrabutylammonium salts of anions were purchased from Sigma–Aldrich. Chloroform ($CHCl_3$), dichloromethane (CH_2Cl_2), acetonitrile (MeCN), petroleum ether, diethyl ether and tetrahydrofuran (THF) were purchased from Cyno-Chem, India. Solvents were dried by conventional methods and distilled under N_2 atmosphere before being used. ^{1}H NMR and ^{13}C NMR spectra were recorded on a Bruker 300 MHz and 75 MHz FT-NMR spectrometers respectively using tetramethylsilane as an internal reference. HRMS measurements were carried out on a Qtof Micro YA263 HRMS instrument. The absorption spectra were recorded with Perkin Elmer Lambda 950 UV–VIS–NIR scanning spectrophotometer and Agilent 8453 UV–vis Spectrometer at 298 K. Elemental analyses for the synthesized ligands were carried out with 2500 series II Elemental Analyser, Perkin Elmer, USA.

X-Ray measurement and structure determination

The crystallographic data and details of data collection for species **1**, complex **2** and complex **3** are given in Table S1(ESI†). In each case, a crystal of suitable size was selected from the mother liquor and immersed in paratone oil, then mounted on the tip of a glass fiber and cemented using epoxy resin. Intensity data for all three crystals were collected using MoKa (λ = 0.7107 Å) radiation on a Bruker SMART APEX diffractometer equipped with CCD area detector at 100 K. The data integration and reduction were processed with SAINT[8a] software. An empirical absorption correction was applied to the collected reflections with SADABS.[8b] Structures were solved by direct method using SHELXTL[9] and are refined on F^2 by the full-matrix least-squares technique using the SHELXL-97[10] program package. Graphics were generated using PLATON[11] and MERCURY 2.2[12] In all cases, non-hydrogen atoms were treated anisotropically. All the hydrogen atoms attached with carbon and nitrogen atoms were geometrically fixed and the hydrogens attached with the oxygen atoms were located in the fourier map and were refined isotropically.

General synthesis procedure

N,*N*′-diaminoguanidine hydrochloride (0.30 g, 2.39 mmol) was taken in 20 ml methanol and it was sonicated for 10 min till it completely dissolved. To this solution the respective aldehyde

Published on 24 January 2011 on http://pubs.rsc.org | doi:10.1039/C0OB00947D
Downloaded by University of Sussex on 06 January 2013

Published on 24 January 2011 on http://pubs.rsc.org | doi:10.1039/C0OB00947D
Downloaded by University of Sussex on 06 January 2013

(1.1 g, 4.78 mmol) was added and it was stirred at r.t for 24 h. Then it was refluxed at 80 °C for 2 h. The product was precipitated out from the solution. It was cooled, filtered and washed with methanol, ether and finally air dried to obtain a solid.

S1. Off white solid. (yield 64%). ^{1}H NMR (300 MHz, DMSO-d_6) δ 12.31 (br, NH), 8.53 (s, 2H), 8.45 (s, 2H), 7.95 (s, 4H), 7.49 (s, 6H); ^{13}C NMR (75 MHz, DMSO-d_6) δ 158.1, 154.0, 138.5, 136.0, 134.0, 133.1; MS (positive ESI): m/z 265.9 $[HL]^+$(100%). Anal. calc. for $C_{15}H_{16}ClN_5$: C, 59.70; H, 5.34; N, 23.21. Found: C, 59.47; H 5.30; N 23.09.

S2. Light yellow solid. (yield 80%). ^{1}H NMR (300 MHz, DMSO-d_6) δ 12.51 (br, NH), 9.42 (s, 1H), 8.64 (s, 1H), 8.44-8.40 (m, 2H), 8.08 (d, J = 8.1 Hz, 1H), 8.03 (d, J = 8.1 Hz, 1H), 7.71–7.58 (m, 3H); ^{13}C NMR (75 MHz, DMSO-d_6) δ 153.0, 147.9, 133.8, 131.7, 131.1, 129.3, 129.0, 127.9, 126.8, 126.7, 126.0, 123.3; MS (positive ESI): m/z 366.2 $[HL]^+$(100%). Anal. calc. for $C_{23}H_{20}ClN_5$: C, 68.74; H, 5.02; N, 17.43. Found: C, 68.31; H 5.10; N 17.41.

S3. Yellow solid. (yield 81%). ^{1}H NMR (300 MHz, DMSO-d_6) δ 12.65 (br, NH), 9.66 (s, 1H), 8.77 (s, 1H), 8.56 (d, J = 8.7 Hz, 2H), 8.18 (d, J = 8.1 Hz, 2H); ^{13}C NMR (75 MHz, DMSO-d_6) δ 152.8, 149.0, 130.8, 129.9, 129.7, 128.9, 127.4, 125.7, 124.9, 124.8; MS (positive ESI): m/z 466.3 $[HL]^+$(100%). Anal. calc. for $C_{31}H_{24}ClN_5$: C, 74.17; H, 4.82; N, 13.95. Found: C, 73.98; H 4.73; N 13.90.

S4. Yellow solid. (yield 72%). ^{1}H NMR (300 MHz, DMSO-d_6) δ 12.30 (br, NH), 9.71 (brs, 1H), 9.05 (d, J = 8.2 Hz, 1H), 8.74 (s, 1H), 8.62 (d, J = 9.4 Hz, 1H), 8.44–8.39 (m, 4H), 8.34–8.26 (m, 2H), 8.17–8.12 (t, 1H); ^{13}C NMR (75 MHz, DMSO-d_6) δ 152.9, 147.5, 133.0, 131.2, 130.5, 129.7, 129.5, 129.2, 127.9, 127.2, 126.8, 126.5, 126.4, 125.6, 125.1, 124.5, 124.2, 122.2; MS (positive ESI): m/z 513.9 $[HL]^+$(100%). Anal. calc. for $C_{35}H_{24}ClN_5$: C, 76.42; H, 4.40; N, 12.73. Found: C, 76.44; H 4.29; N 12.61.

S5. Yellow white solid. (yield 80%). ^{1}H NMR (300 MHz, DMSO-d_6) δ 12.16 (br, NH), 8.38 (s, 1H), 7.88 (d, J = 8.6 Hz, 2H), 7.02 (d, J = 8.6 Hz, 2H), 3.82 (s, 3H); ^{13}C NMR (75 MHz, DMSO-d_6) δ 161.4., 152.6, 148.5, 129.6, 125.9, 114.26, 55.42; MS (positive ESI): m/z 326.1 $[HL]^+$(100%). Anal. calc. for $C_{17}H_{20}ClN_5O_2$: C, 56.43; H, 5.57; N, 19.36. Found: C, 56.07; H 5.24; N 19.25.

S6. White solid. (yield 70%). ^{1}H NMR (300 MHz, DMSO-d_6) δ 12.7 (br, NH), 8.60 (s, 2H), 8.34 (s, 2H); ^{13}C NMR (75 MHz, DMSO-d_6) δ 153.3, 146.8, 143.4, 138.4, 136.1, 109.3; MS (positive ESI): m/z 445.9 $[L]^+$. Anal. calc. for $C_{15}H_6ClF_{10}N_5$: C, 37.40; H, 1.26; N, 14.54. Found: C, 37.21; H 1.32; N 14.39.

S7. Off white solid. (yield 81%). ^{1}H NMR (300 MHz, DMSO-d_6) δ 12.76 (br, NH), 8.88 (s, 1H), 8.77 (s, 1H), 8.49 (d, J = 8.1 Hz, 1H), 8.12 (d, J = 8.4 Hz, 1H), 7.86 (t, J = 9.3 Hz, 1H), 7.74 (t, J = 9.5 Hz, 1H); ^{13}C NMR (75 MHz, DMSO-d_6) δ 153.6., 148.9, 145.3, 134.2, 131.9, 129.4, 128.2, 125.3; MS (positive ESI): m/z 356.1 $[HL]^+$(100%). Anal. calc. for $C_{15}H_{14}ClN_7O_4$: C, 45.99; H, 3.60; N, 25.03. Found: C, 46.06; H 3.56; N 25.35.

S8. Yellow solid. (yield 85%). ^{1}H NMR (300 MHz, DMSO-d_6) δ 12.59 (br, NH), 8.83 (s, 1H), 8.81 (s, 1H), 8.75 (s, 1H); 8.39 (d, J = 4.8 Hz, 1H), 8.30 (d, J = 5.1 Hz, 1H), 7.78 (t, J = 9.6 Hz, 1H) ^{13}C NMR (75 MHz, DMSO-d_6) δ 148.9, 135.7, 134.7, 130.8, 125.5, 122.5; MS (positive ESI): m/z 355.9 $[HL]^+$(100%). Anal. calc. for $C_{15}H_{14}ClN_7O_4$: C, 45.99; H, 3.60; N, 25.03. Found: C, 46.05; H 3.33; N 24.70.

S9. Yellow solid. (yield 75%). ^{1}H NMR (300 MHz, DMSO-d_6) δ 8.69 (br, NH), 8.53 (s, 2H), 8.29 (d, 4H), 8.21 (d, J = 6.76 Hz, 4H); ^{13}C NMR (75 MHz, DMSO-d_6) δ 154.1, 148.6, 146.8, 140.1, 129.2, 124.3; MS (positive ESI): m/z 355.8 $[HL]^+$(100%). Anal. calc. for $C_{15}H_{14}ClN_7O_4$: C, 45.99; H, 3.60; N, 25.03. Found: C, 45.86; H 3.49; N 24.99.

S10. Greenish white solid (yield 70%). ^{1}H NMR (300 MHz, DMSO-d_6) δ 11.83 (s, 1H), 11.61 (br, NH), 8.58 (s, 1H), 8.37 (d, J = 7.6 Hz, 1H), 7.98 (s, 1H), 7.89 (s, 1H), 7.49 (d, J = 7.5 Hz, 1H), 7.28–7.18 (m, 2H); ^{13}C NMR (75 MHz, DMSO-d_6) δ 152.2, 146.9, 137.7, 132.7, 124.5, 123.4, 122.9, 121.3, 112.5, 111.2; MS (positive ESI): m/z 343.8 [L] (100%). Anal. calc. for $C_{19}H_{18}ClN_7$: C, 60.08; H, 4.78; N, 25.81. Found: C, 59.91; H 4.81; N 25.80.

Conclusions

In summary, we have synthesized a new series of guanidinium chloride derivatives (**S1–S10**) based on increasing aromaticity, induction effect, positional isomeric effect and NIR sensing ability of the substituted functional group attached to the guanidinium moiety. This series of sensor molecules shows selective colour changes with fluoride and in most of the cases no change in colour or absorption spectra are observed with closely related basic anions like acetate and phosphate. The spectrum of colour change across the series with the fluoride shows a pattern of colour changes as well as absorption spectra which could be utilized for its confirmed detection. Interestingly, we also demonstrate that one of the sensor molecules can be utilized to differentiate fluoride, acetate and dihydrogen phosphate by colourimetric and optical studies. Further, single crystal X-ray structural analyses supports –NH deprotonation in the presence of highly basic F^- and 1 : 1 binding in the presence of less basic anion benzoate.

Acknowledgements

P.G. gratefully acknowledges the Department of Science and Technology (DST), New Delhi for financial support. P.B. would like to acknowledge CSIR, India for SRF. X-ray crystallography study is performed at the DST-funded National Single Crystal X-ray Diffraction Facility at the Department of Inorganic Chemistry, IACS.

Notes and references

1 (*a*) K. L. Kirk, *Biochemistry of the Halogens and Inorganic Halides*, Plenum Press, New York, 1991, p 58; (*b*) *Supramolecular Chemistry of Anions*, A. Bianchi, K. Bowman-James and E. García-España, ed., Woley-VCH, New York, 1997; (*c*) P. D. Beer and P. A. Gale, *Angew. Chem., Int. Ed.*, 2001, **40**, 486; (*d*) J. L. Sessler, P. A. Gale and W.-S. Cho, *Anion Receptor Chemistry*, The Royal Society of Chemistry, Cambridge, UK, 2006; (*e*) M. Cametti and K. Rissanen, *Chem. Commun.*, 2009, 2809; (*f*) P. A. Gale, S. E. García-Garrido and J. Garric, *Chem. Soc. Rev.*, 2008, **37**, 151–190; (*g*) T. Gunnlaugsson, A. P. Davis, J. E. O'Brien and M. Glynn, *Org. Lett.*, 2002, **4**, 2449; (*h*) J. Shao, H. Lin, M. Yu, Z. Cai and H. Lin, *Talanta*, 2008, **75**, 551.

2 Representative examples: (*a*) P. D. Beer and F. Szemes, *J. Chem. Soc., Chem. Commun.*, 1995, 2245; (*b*) P. A. Gale, J. L. Sessler, V. Král and V. Lynch, *J. Am. Chem. Soc.*, 1996, **118**, 5140; (*c*) P. D. Beer, F. Szemes, V. Balzani, C. M. Sala, M. G. B. Drew, S. W. Dent and M. Maestri, *J.*

 This journal is © The Royal Society of Chemistry 2011

View Article Online

Am. Chem. Soc., 1997, **119**, 11864; (*d*) C. B. Black, B. Andrioletti, A. C. Try, C. Ruiperez and J. L. Sessler, *J. Am. Chem. Soc.*, 1999, **121**, 10438; (*e*) T. Gunnlaugsson, A. P. Davis and M. Glynn, *Chem. Commun.*, 2001, 2556; (*f*) M. Vázquez, L. Fabbrizzi, A. Taglietti, R. M. Pedrido, A. M. González-Noya and M. R. Bermejo, *Angew. Chem., Int. Ed.*, 2004, **43**, 1962; (*g*) D. A. Jose, D. K. Kumar, B. Ganguly and A. Das, *Org. Lett.*, 2004, **6**, 3445; (*h*) D. Esteban-Gómez, L. Fabbrizzi and M. Licchelli, *J. Org. Chem.*, 2005, **70**, 5717; (*i*) E. J. Cho, B. J. Ryu, Y. J. Lee and K. C. Nam, *Org. Lett.*, 2005, **7**, 2607; (*j*) D. Curiel, A. Cowley and P. D. Beer, *Chem. Commun.*, 2005, 136; (*k*) D. Aldakov, M. A. Palacios and P. Anzenbacher, Jr, *Chem. Mater.*, 2005, **17**, 5238; (*l*) X. He, S. Hu, K. Liu, Y. Guo, J. Xu and S. Shao, *Org. Lett.*, 2006, **8**, 333; (*m*) J. L. Sessler, D.-G. Cho and V. Lynch, *J. Am. Chem. Soc.*, 2006, **128**, 16518; (*n*) T. Mizuno, W.-H. Wei, L. R. Eller and J. L. Sessler, *J. Am. Chem. Soc.*, 2006, **124**, 1134; (*o*) L. S. Evans, P. A. Gale, M. E. Light and R. Quesada, *Chem. Commun.*, 2006, 965; (*p*) J. Yoo, M.-S. Kim, S.-J. Hong, J. L. Sessler and C.-H. Lee, *J. Org. Chem.*, 2009, **74**, 1065; (*q*) F. Han, Y. Bao, Z. Yang, T. M. Fyles, J. Zhao, X. Peng, J. Fan, Y. Wu and S. Sun, *Chem.–Eur. J.*, 2007, **13**, 2880; (*r*) P. Bose and P. Ghosh, *Chem. Commun.*, 2010, **46**, 2962.

3 M. Boiocchi, L. D. Boca, D. Esteban-Gómez, L. Fabbrizzi, M. Licchelli and E. Monzani, *Chem.–Eur. J.*, 2005, **11**, 3097.

4 (*a*) M. Onda, K. Yoshihara, H. Koyano, K. Ariga and T. Kunitake, *J. Am. Chem. Soc.*, 1996, **118**, 8524; (*b*) A. Metzger, V. M. Lynch and E. V. Anslyn, *Angew. Chem., Int. Ed. Engl.*, 1997, **36**, 862; (*c*) F. P. Schmidtchen and M. Berger, *Chem. Rev.*, 1997, **97**, 1609; (*d*) C. Schmuck and J. Lex, *Org. Lett.*, 1999, **1**, 1779; (*e*) M. Fibbioli, M. Berger, F. P. Schmidtchen and E. Pretsch, *Anal. Chem.*, 2000, **72**, 156; (*f*) J. Raker and T. E. Glass, *J. Org. Chem.*, 2002, **67**, 6113; (*g*) S. L. Tobey and E. V. Anslyn, *J. Am. Chem. Soc.*, 2003, **125**, 14807; (*h*) C. Schmuck and L. Geiger, *J. Am. Chem. Soc.*, 2004, **126**, 8898; (*i*) C. Schmuck and M. Schwegmann, *J. Am. Chem. Soc.*, 2005, **127**, 3373; (*j*) K. A. Schug and W. Lindner, *Chem. Rev.*, 2005, **105**, 67; (*k*) C. Schmuck, *Coord. Chem. Rev.*, 2006, **250**, 3053; (*l*) P. Blondeau, M. Segura, R. P. -Fernández and J. Mendoza, *Chem. Soc. Rev.*, 2007, **36**, 198; (*m*) C. Schmuck and V. Bickert, *J. Org. Chem.*, 2007, **72**, 6832; (*n*) V. D. Jadhav and F. P. Schmidtchen, *J. Org. Chem.*, 2008, **73**, 1077; (*o*) M. P. Coles, *Chem. Commun.*, 2009, 3659.

5 (*a*) K. Niikura, A. Metzger and E. V. Anslyn, *J. Am. Chem. Soc.*, 1998, **120**, 8533; (*b*) S. C. McCleskey, A. Metzger, C. S. Simmons and E. V. Anslyn, *Tetrahedron*, 2002, **58**, 621; (*c*) C. Schmuck and M. Schwegmann, *Org. Biomol. Chem.*, 2006, **4**, 836.

6 (*a*) F. Otón, A. Tárraga and Pedro Molina, *Org. Lett.*, 2006, **8**, 2107; (*b*) F. Otón, A. Espinosa, A. Tárraga, C. R. Arellano and P. Molina, *Chem.–Eur. J.*, 2007, **13**, 5742; (*c*) Y. Sun, C. Zhong, R. Gong, H. Mu and Enqin Fu, *J. Org. Chem.*, 2009, **74**, 7943.

7 (*a*) S. Rensing, M. Arendt, A. Springer, T. Grawe and T. Schrader, *J. Org. Chem.*, 2001, **66**, 5814; (*b*) P. B. Crowley1 and A. Golovin, *Proteins: Struct., Funct., Bioinf.*, 2005, **59**, 231; (*c*) X. Wang, O. V. Sarycheva, B. D. Koivisto, A. H. McKie and F. Hof, *Org. Lett.*, 2008, **10**, 297.

8 (*a*) *SAINT and XPREP*, 5.1 ed., Siemens Industrial Automation Inc., Madison, WI, 1995; (*b*) G. M. Sheldrick, *SADABS, empirical absorption Correction Program*, University of Göttingen, Göttingen, Germany, 1997 .

9 G. M. Sheldrick, *SHELXTL Reference Manual: Version 5.1*, Bruker AXS, Madison, WI, 1997.

10 G. M. Sheldrick, *SHELXL-97: Program for Crystal Structure Refinement*, University of Göttingen, Göttingen, Germany, 1997.

11 A. L. Spek, *PLATON-97*, University of Utrecht, Utrecht, The Netherlands, 1997.

12 Mercury 2.2 supplied with Cambridge Structural Database, CCDC, Cambridge, UK.

Published on 24 January 2011 on http://pubs.rsc.org | doi:10.1039/C0OB00947D
Downloaded by University of Sussex on 06 January 2013